The Effect of Supercooling on Crystallization of Cocoa Butter–Vegetable Oil Blends

David Pérez-Martínez[a], C. Alvarez-Salas[a], J.A. Morales-Rueda[a], J.F. Toro-Vazquez[b,*], M. Charó-Alonso[b], and E. Dibildox-Alvarado[b]

[a]Facultad de Química, Departamento de Investigación y Posgrado en Alimentos (PROPAC), Universidad Autónoma de Querétaro, Querétaro, México, and [b]Facultad de Ciencias Químicas, Centro de Invesigación y Estudios de Posgrado (CIEP), Universidad Autónoma de San Luis Potosí, San Luis Potosí 78210, México

ABSTRACT: The solid fat content (SFC), Avrami index (*n*), crystallization rate (*z*), fractal dimension (*D*), and the pre-exponential term [log(γ)] were determined in blends of cocoa butter (CB) with canola oil or soybean oil crystallized at temperatures (T_{Cr}) between 9.5 and 13.5°C. The relationship of these parameters with the elasticity (G') and yield stress (σ*) values of the crystallized blends was investigated, considering the equilibrium melting temperature ($T_M°$) and the supercooling (i.e., $T_{Cr}° - T_M°$) present in the blends. In general, supercooling was higher in the CB/soybean oil blend [$T_M°$ = 65.8°C (±3.0°C)] than in the CB/canola oil blend [$T_M°$ = 33.7°C (±4.9°C)]. Therefore, under similar T_{Cr} values, higher SFC and *z* values ($P < 0.05$) were obtained with the CB/soybean oil blend. However, independent of T_{Cr} TAG followed a spherulitic crystal growth mechanism in both blends. Supercooling calculated with melting temperatures from DSC thermograms explained the SFC and *z* behavior just within each blend. However, supercooling calculated with $T_M°$ explained both the SFC and *z* behavior within each blend and between the blends. Thus, independent of the blend used, SFC described the behavior of G'_{eq} and σ* and pointed out the presence of two supercooling regions. In the lower supercooling region, G'_{eq} and σ* decreased as SFC increased between 20 and 23%. In this region, the crystal network structures were formed by a mixture of small β′ crystals and large β crystals. In contrast, in the higher supercooling region (24 to 27% SFC), G'_{eq} and σ* had a direct relationship with SFC, and the crystal network structure was formed mainly by small β′ crystals. However, we could not find a particular relationship that described the overall behavior of G'_{eq} and σ* as a function of *D* and independent of the system investigated.

Paper no. J10993 in *JAOCS 82*, 471–479 (July 2005).

KEY WORDS: Avrami, cocoa butter, crystallization, elastic modulus, polymorphism, rheometry, yield stress.

In crystallized lipid systems, the solid-to-liquid ratio (1) and the geometric organization of the crystal network (2,3) determine much of their rheology, which in turn is associated with functional properties in products such as margarine, butter, confectionary coatings, and fillings. TAG crystallization may occur once the system is under supercooling conditions, since this thermodynamic force drives the formation of a solid in the liquid phase. In polymers, supercooling has been defined as the difference between the temperature of crystallization, T_{Cr}, and the equilibrium melting temperature, $T_M°$. $T_M°$ is the hypothetical melting temperature of an assembly of molecules of infinite size, so that the surface effect on the melting temperature is negligible (4). An additional assumption is that at $T_M°$ the structural organization of such crystals is in equilibrium with the molecules in the melt. Thus, aggregations of molecules without the correct 3-D arrangement to develop a stable crystal, and therefore small crystals, will melt below $T_M°$ (4). Within this framework, $T_M°$ may occur at high temperatures if the molecules in the melt are oriented to an appreciable extent. Consequently, $T_M°$ is a constant that describes the structural organization of the molecules in the melt and is a parameter specific for each particular system but independent of the experimental conditions. In contrast, the experimental melting temperature depends on both the system under evaluation and the experimental conditions used. Supercooling determined using experimental melting temperature values can be used to evaluate the effect of different crystallization conditions (i.e., different T_{Cr} values) within a particular system. The comparison of crystallization conditions used in different systems requires the use of supercooling calculated with $T_M°$, previous determination of $T_M°$ in each system in particular. Although the $T_M°$ concept was developed for polymers, this principle also applies for the true m.p. of pure compounds of nonpolymeric nature (i.e., nonionic molecules, ionic or metallic crystals) (4). Thus, our group has applied this concept to investigate the crystallization process of vegetable oil blends, specifically, of palm stearin in sesame oil (5).

As previously discussed, the $T_M°$ concept is associated with the extent of crystal perfection required by the hypothetical assembly of molecules of infinite size with a melting temperature equal to $T_M°$. Based on this definition, $T_M°$ also must be associated with the molecular compatibility among the major families of compounds, that is, TAG present in a particular system (i.e., pure TAG, vegetable oil, or a blend of vegetable oils). Therefore, with pure TAG (i.e., PPP, OOO, POP, where P = palmitic acid and O = oleic acid) $T_M°$ would achieve its maximum value. However, in a mixture of TAG families, such as in a vegetable oil or a blend of vegetable oils, $T_M°$ might be associated with the molecular compatibility among the major families of TAG present. In a vegetable oil, the greater the molecular compatibility

*To whom correspondence should be addressed at Facultad de Ciencias Químicas–CIEP, Av. Dr. Manuel Nava 6, Zona Universitaria, San Luis Potosí, SLP 78210, México. E-mail: toro@uaslp.mx

of a particular family or group of TAG with other TAG molecules in the melt, the more the original structural organization of the pure TAG is altered. Modification of the extent of crystal perfection is required to develop the hypothetical assembly of molecules of infinite size. As a result, a lower T_M° is observed in a vegetable oil or a blend of vegetable oils than in pure TAG. In contrast, the lower the compatibility (i.e., solubility) is of a particular family or group of TAG with other TAG molecules in a vegetable oil, the more the original structural organization of the pure TAG is preserved, resulting in higher T_M° values. Consequently, the molecular relationships among TAG families determine the thermodynamic conditions that drive the formation of a solid in a liquid phase such as a vegetable oil or vegetable oil blend.

In this work, blends of cocoa butter (CB) with canola oil or soybean oil were used as model systems with the objective of evaluating the rheological properties of elasticity and yield stress of the crystallized blends and their relationships with the solid-phase parameters of solid fat content (SFC) and fractal dimension. Although oleic and linoleic acids are the major FA in both vegetable oils, soybean oil has a higher ratio of linoleic (43–56%) to oleic acid (15–33%) than canola oil (20–21% linoleic acid, 60–70% oleic acid) (6–8). Thus, the molecular compatibilities between soybean oil TAG and the TAG of CB must be different from the ones between the TAG of CB and canola oil. Subsequently, T_M° ought to be different in each CB/vegetable oil blend, and for similar crystallization temperatures different supercooling conditions would exist. Therefore, the relationships between solid-phase parameters and rheological properties of crystallized systems were studied under similar crystallization temperatures but different supercooling conditions.

MATERIALS AND METHODS

Blends of CB in canola or soybean oil were prepared at ratios between 0 and 100% CB (% wt/vol). The CB, previously vacuum-filtered through Whatman paper no. 5, was melted (80°C for 20 min) and the corresponding proportion weighed into a 100-mL volumetric flask. The flask was filled to the mark with canola or soybean oil and the blend was stored (4°C) under nitrogen in the dark.

The TAG profiles of CB and the vegetable oils were determined by HPLC using a light-scattering detector. Sample elution was carried out at room temperature through two Nova Pak C_{18} columns (3.9 × 150 mm; Waters, a division of Millipore Co., Milford, MA) connected in series using a solvent gradient of acetonitrile/dichloromethane from 70:30 to 30:70. The gradient program was applied over 1 h using two mixtures (90:10 and 10:90) of acetonitrile/dichloromethane. The assignment of TAG peaks was based on the retention time of TAG standards (Supelco, Bellefonte, PA; Sigma Chemical Co., St. Louis, MO). The area under each peak in the chromatogram was calculated and the TAG concentration was determined as a percentage from the total area. At least duplicate determinations were done.

Dynamic calorimetric analyses were done in a DSC instrument calibrated as previously indicated (9). Samples (≈12 mg) of the blends (0–100% CB/vegetable oil) were sealed in aluminum pans and held at 80°C for 20 min. Then the system was cooled (10°C/min) from 80 to −50°C. After 1 min at −50°C, the melting thermogram was obtained by heating (5.0°C/min). The difference in heat capacity between the reference and sample cells was partly compensated for by using in the reference cell a sealed pan with the same weight of inert material (i.e., aluminum) as CB/vegetable oil blend in the sample pan (≈12 mg). The onset of crystallization (T_o) was calculated from the crystallization thermogram with the DSC software. The end of melting (T_e) was calculated from the melting thermograms by using the first derivative of the heat capacity of the sample. T_e was defined as the temperature at which the first derivative of the heat capacity of the last endotherm returned to the baseline. T_o and T_e for each CB blend were plotted as a function of CB concentration. The blend with the lowest concentration of CB still following a linear decrease in T_o and T_e (i.e., ideal solution behavior) as the proportion of soybean or canola oil increased in the blend was used as a model system for further crystallization studies.

For the isothermal DSC analysis, a sample (≈12 mg) of the blend with the CB concentration selected as described above was sealed in an aluminum pan and held for 20 min at 80°C. The system was cooled at 1°C/min until it attained a particular T_{Cr}. After completion of the crystallization exotherm (i.e., heat capacity returned to the baseline), the system was left for an additional 30 min and then the melting thermogram was determined by heating (5°C/min). The melting temperature at the peak (T_M') of the endotherm was determined using the first derivative of the heat capacity. T_M' was considered the experimental melting temperature of the polymorph crystallized at a particular T_{Cr}. The equilibrium melting temperature (T_M°) for each blend was determined with the T_M' values following the procedure of Hoffman and Weeks (4) as described previously (5). In brief, for the CB/canola oil and the CB/soybean oil blends the corresponding linear relationship between T_{Cr} and T_M' was established. Thus, the experimental T_{Cr} vs. T_M' plot provided a linear relationship whose crossing point with the theoretical equilibrium line ($T_{Cr} = T_M'$) represented T_M°. For each CB/vegetable oil blend, three independent determinations were done.

The SFC (%) of the CB blends was determined by pulsed NMR with a Bruker Minispec model mq20 equipped with a jacketed measuring probe connected to a programmable temperature bath set to a cooling rate of 1°C/min (±0.1°C/min). Samples (4 mL) of the blends were heated (80°C for 20 min) in NMR tubes (10 mm × 20 cm) and then cooled in the bath until attaining 40°C. The circulation of the cooling fluid to the jacketed measuring probe was then opened and the NMR tube was inserted in the measuring probe to continue cooling until attaining the corresponding T_{Cr}. The SFC readings as a function of isothermal crystallization time (SFC_t) were recorded by the equipment software until 30 min after achieving a sustained plateau in the measurements. These values were considered the

maximum or equilibrium SFC (SFC_{eq}). With the Avrami equation (Eq. 1) as the crystallization model, the SFC values were used to calculate the fractional crystallization, F, as a function of isothermal crystallization time, t, as $F = SFC_t/SFC_{eq}$. The Avrami index (n) and the crystallization rate constant (z) were determined by fitting Equation 1 through the nonlinear estimation procedure available in STATISTICA (v. 6.0; StatSoft, Inc., Tulsa, OK). In all cases at least two independent determinations were done at each T_{Cr}:

$$1 - F = \exp(-zt^n) \quad [1]$$

A mechanical spectrometer equipped with 50-mm-diameter parallel-plate geometry was used for the elasticity (G') and the yield stress (σ^*) measurements. Temperature control was achieved by a Peltier system located in the base of the measurement geometry. The melted blend (80°C) was applied on the base of the plate, avoiding bubble formation, and the superior plate was positioned on the sample surface using the auto-gap function available in the rheometer software (1 mm). The sample was first heated (80°C for 20 min) and then cooled (1°C/min) while applying a constant strain (1 mrad) until achieving the corresponding T_{Cr}. The G' and the σ^* for each blend at the different T_{Cr} values were determined by applying a strain sweep (0.025% up to 5%) to the crystallized systems after times equivalent to the ones used for the SFC_{eq}. From the log-log plots of G', G'' vs. strain (%) the elasticity at equilibrium (G'_{eq}) was determined within the linear viscoelastic region (LVR). In the same way, the σ^* was determined from the log-log plot of shear stress vs. strain (%) at the corresponding upper limit of strain within the LVR.

The measurement of the dimensionality of the TAG crystal network was based on the weak-link regime for colloidal dispersions (i.e., systems with a high volume fraction of solids) (2). In these systems, G' increases as a function of the volume fraction of solid fat (ϕ) following Equations 2 and 3, where m depends on the mass fractal dimension (D), and the pre-exponential term (γ) is a constant independent of ϕ but dependent on the size of the primary particles and on the interactions between them (i.e., polymorphic nature of the crystals) (2):

$$G' = \gamma\phi^m \quad [2]$$

$$\log(G') = \log(\gamma) + m[\log(\phi)] \quad [3]$$

$$m = 1/(3 - D) \quad [4]$$

Thus, conical glass tubes (15 × 110 mm) containing 4 mL of the sample were cooled in the programmable temperature bath using the same procedure as for SFC. At specific crystallization times under isothermal conditions, the sample contained in one tube was gently poured on the base of the plate of the rheometer. The sample was handled with care to avoid disruption of the original structure and bubble formation. The superior plate of the rheometer was positioned on the sample surface using the auto-gap function, and an oscillatory strain sweep was applied to the sample using a logarithmic ramp between 0.001 and 10% at a constant angular frequency (1 rad/s). Twenty rheological measurements in 2.5 min were acquired by the rheometer software, and the G' value was determined within the LVR. The same procedure was followed for several crystallization times. Then log-log plots of G' vs. SFC, both values having been obtained at the same crystallization time, were obtained to calculate D and $\log(\gamma)$ from Equations 3 and 4, assuming that $SFC \approx \phi$. Duplicate determinations were done in each case.

Polarized light microscopy (PLM) was used to examine the morphology of the crystallized systems. To guarantee a uniform sample thickness, two cover slips were glued to a glass microscope slide with a distance of 2.2 cm between them. The sample (80°C) was placed within this gap of a preheated (80°C) glass slide, and a glass cover slip was placed over the sample such that it rested on the glued cover slips. This provided a uniform sample thickness of ≈0.16 mm. After 30 min at 80°C, the system was cooled (1°C/min) to T_{Cr}. Photomicrographs and video as a function of time were obtained of the slide, connected to a temperature control station, with a polarized light microscope equipped with a color video camera.

RESULTS AND DISCUSSION

Selection of the model system for crystallization studies. The TAG profile for CB showed that the symmetrical saturate-unsaturate-saturate (SUS)-type TAG (i.e., StOSt, POSt, and POP, where St = stearic acid, O = oleic acid, P = palmitic acid) added up to ≈87.9%, whereas diunsaturated asymmetrical TAG (i.e., POO and StOO) were ≈5.6% and trisaturated TAG (i.e., StStSt, PStSt, and PPSt) were ≈0.73%. In contrast, canola and soybean oils had high concentrations of triunsaturated TAG, ≈87.3 and ≈59.3%, respectively. The major TAG in canola oil were OOO, LOO, and OLnO (where L = linoleic acid and Ln = linolenic acid), whereas in the soybean oil they were LLL, LLO, and LOO. Because of the steric nature of the *cis* unsaturation present in the highly unsaturated TAG of canola and soybean oils, major TAG components of CB might be segregated from the highly unsaturated TAG phase of canola and soybean oil during the crystallization process. Thus, the T_o and T_e plot as a function of CB concentration in the blends showed an ideal solution-type behavior in the interval between 30 and 100% CB, i.e., T_o and T_e decreased linearly as soybean or canola oil diluted the TAG from CB (data not shown). This behavior showed that in the presence in the blends of between 30 and 100% of CB, no mixed crystals were developed between the TAG of CB and the TAG of canola or soybean oil. However, below 30% CB concentration T_o and T_e did not follow this behavior (data not shown). At CB concentrations lower than 30%, some TAG from canola or soybean oil and TAG from CB apparently produced mixed crystals, resulting in crystals with T_o and T_e values lower than the ones for CB crystals. The formation of mixed crystals thus was dependent on the CB concentration in the blends. Similar behavior has been reported in other TAG systems, e.g., blends of tripalmitin or tristearin in triolein (10) and blends of tripalmitin or palm stearin in sesame oil (11). In our results, the 30% CB in canola and soybean oil

had the lowest concentration of CB that still provided crystallization and melting properties mainly associated with TAG from CB. The corresponding T_{Cr} values used in the isothermal crystallization studies were 9.5, 10.5, 11.5, and 13.0°C for the 30% CB/canola oil and 10, 11, 12, and 13.5°C for the 30% CB/soybean oil. These T_{Cr} values were selected based on the dynamic crystallization and melting thermograms (data not shown).

Characterization of the CB/vegetable oil blends by DSC and determination of $T_M°$. The isothermal crystallization of both CB/vegetable oil blends showed behavior quite similar to that observed for pure CB (12). Based on the time–temperature X-ray diffraction state diagrams for pure CB obtained by van Malssen *et al.* (13), we assigned the first exotherm to the α polymorph and the second exotherm to the β′ polymorph. As previously described, TAG from CB were the only ones crystallizing in the 30% CB/vegetable oil blends investigated. Therefore, as in pure CB, the first and second exotherms obtained during isothermal crystallization of the blends were also assigned to the α and β′ polymorphs, respectively. On the other hand, the corresponding melting thermograms showed the presence of two endotherms, the first assigned to β′ melting (T_M') and the second to the β polymorph melting (T_{P2}) (Fig. 1B for 30% CB/canola; 30% CB/soybean not shown). This last polymorph was developed probably through an α→β polymorphic transition. The presence of the α polymorph was necessary for the formation of β crystals *via* the α→β′→β polymorphic transition since TAG from CB do not nucleate directly from the melt into the β phase. Additionally, Gibon *et al.* (14) had shown that the β′ polymorph of symmetrical TAG, like the ones present in CB, is less prone to β′→β polymorphic transition when β′ crystallizes directly from the melt than when crystallizing *via* the α→β′→β process. Based on these results, only T_M', the temperature at the peak of first endotherm (i.e., β′ melting), was considered in the determination of $T_M°$, since the second endotherm (T_{P2}) was associated with the melting of crystals derived from a polymorphic transition (β) (Fig. 1B). Thus, the $T_M°$ for the CB/canola oil blends was 33.7°C (±4.9°C) whereas the $T_M°$ for the CB/soybean oil blends was 65.8°C (±3.0°C) (Fig. 2). In the liquid phase of the blends, the major TAG present in soybean oil (e.g., 21.4% LLL, 21.1% LLO, and 14.5% LLP) seemed to have a lower extent of molecular compatibility with the symmetrical SUS type and the saturated TAG from CB than the major TAG present in canola oil (e.g., 39.4% OOO and 26.1% LOO). This occurs mainly because of the higher degree of unsaturation present in soybean oil TAG in comparison with TAG of canola oil. Then, although similar T_{Cr} values were used, supercooling [measured as ($T_{Cr} - T_M°$)] was higher for the CB/soybean oil than for the CB/canola oil.

Supercooling and its effect on SFC_{eq}, the Avrami index, and the crystallization rate constant. The same concentration of CB was present in both blends. Independent of the blend, higher SFC_{eq} values were expected at the lower T_{Cr} investigated (i.e., 9.5°C in the CB/canola oil blend). However, this was not the case. Thus, with the CB/canola oil blend, the highest SFC_{eq} value was attained at 9.5°C with an SFC_{eq} of 24.4% (±0.5) (Table 1). In contrast, with the CB/soybean oil blend the highest SFC_{eq} values were achieved at the T_{Cr} values of 10 and 11.0° (Table 1), with an average SFC_{eq} of 25.8% (±0.8). This SFC_{eq} value was statistically greater ($P < 0.05$) than the SFC_{eq} obtained at 9.5°C with the CB/canola oil blend despite the higher T_{Cr} values (i.e., 10 and 11.0°C) used with the CB/canola oil blends. By the same token, the SFC_{eq} obtained at a T_{Cr} of 13.5°C [22.1% (±0.4)] with the CB/soybean oil blend was statistically greater ($P < 0.05$) than the value obtained at a T_{Cr} of 13.0°C with the CB/canola oil blend [20.7% (±0.4)]. It is important to point out that supercooling, calculated with the corresponding T_e and T_{P2} values for each blend [i.e., ($T_{Cr} - T_e$) or ($T_{Cr} - T_{P2}$)] data not shown], explained the increase in SFC_{eq} as T_{Cr} decreased within each CB blend (Table 1). However, this supercooling did not explain the higher SFC_{eq} obtained with the CB/soybean oil blend in comparison with the SFC_{eq} obtained at similar T_{Cr} values with the CB/canola oil. On the other hand, the supercooling calculated as ($T_{Cr} - T_M°$) showed that under similar T_{Cr} conditions, supercooling was higher in the CB/soybean oil blends, which in turn achieved the highest SFC_{eq} values. Thus, supercooling calculated as ($T_{Cr} - T_M°$) explained both the increase in SFC_{eq} values as T_{Cr} decreased

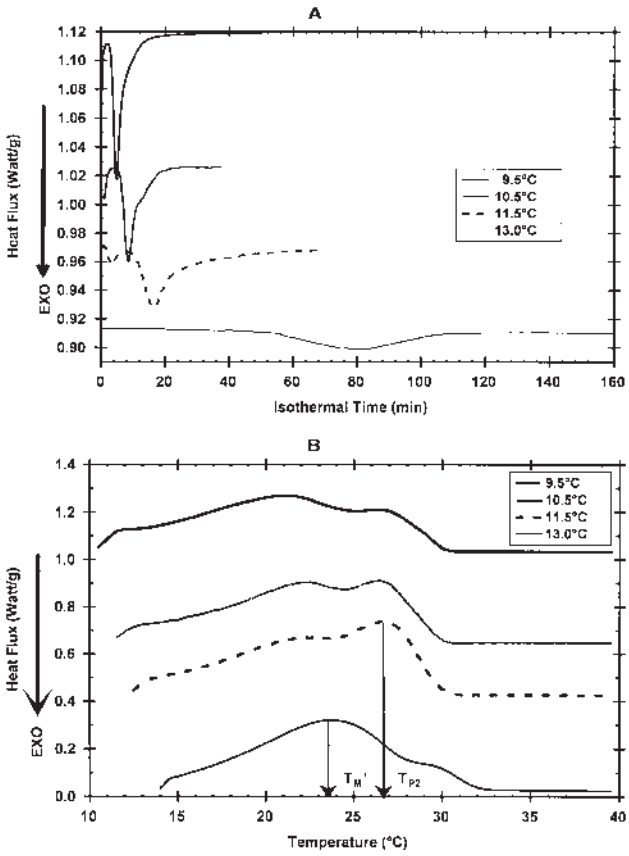

FIG. 1. Isothermal crystallization (A) and corresponding melting thermograms (B) for the 30% cocoa butter (CB)/canola oil blend. The arrows in (B) show the peak temperature (T_M') of the endotherm used in calculating the equilibrium melting temperature ($T_M°$), and the peak temperature of the endotherm associated with the melting of β crystals (T_{P2}). The crystallization temperatures are shown in the legend.

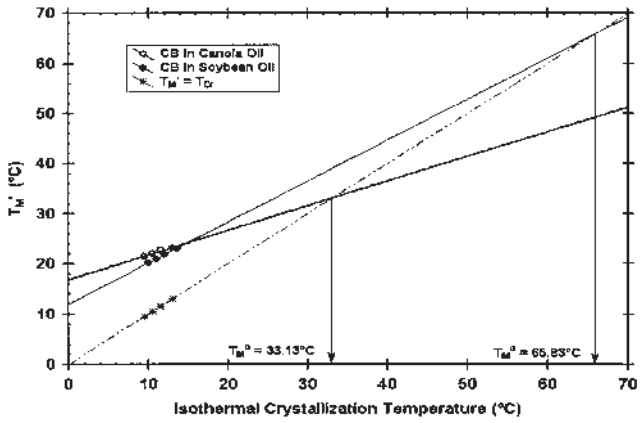

FIG. 2. Determination of the equilibrium melting temperature, $T_M°$, for the 30% cocoa butter (CB)/canola oil blend and the 30% CB/soybean oil blend. The corresponding $T_M°$ values are shown. T_{CR}, crystallization temperature.

within each blend (Table 1) and the higher SFC_{eq} values achieved by the blend with the greater level of supercooling (i.e., CB/soybean oil blend, $T_M° = 65.83°C$).

Regarding the crystallization process of CB in the vegetable oils, the *n* value from Avrami's theory determines the dimensionality of the crystal growth when limited or no crystal impingement occurs. PLM photomicrographs of crystals developed at two crystallization times in the CB/soybean oil blend at 10.0°C are shown in Figures 3A and 3B, and for the CB/canola oil blend at 13.0°C in Figures 4A and 4B. No crystal impingement occurred at crystallization times where the Avrami exponent was determined (i.e., Figs. 3A and 4A). Additionally, visual analysis of the video recordings showed that instantaneous nucleation occurred at the lower T_{Cr} values used in each blend, i.e., 9.5 and 10.5°C in the CB/canola oil blend, and at 10.0 and 11.0°C in the CB/soybean oil blend. At the other T_{Cr} values, sporadic nucleation occurred (Table 1). With this information and considering that *n* is a function of the time dependence of nucleation (i.e., sporadic or instantaneous) and the dimensionality of the crystal growth process (15), the *n* values (Table 1) indicate that, independent of the T_{Cr} used, TAG of CB followed a spherulitic crystal growth mechanism in both blends. The fractional values obtained in the determination of *n* (Table 1) might indicate the simultaneous development of at least two types of crystals, as observed in some blends under some crystallization conditions (i.e., CB/canola oil blend at 13.0°C, Fig. 4B). In contrast to *n*, the SFC_{eq} was measured after long times of crystallization where crystal impingement was widespread in the crystallized systems (Figs. 3B and 4B). Figures 3 and 4 show PLM photomicrographs of crystallized CB/soybean oil blends (11.0°C, Fig. 3C; 12.0°C, Fig. 3D; 13.5°C, Fig. 3E) and CB/canola oil blends (9.5°C, Fig. 4C; 10.5°C, Fig. 4D; 11.5°C, Fig. 4E) corresponding to crystallization times where SFC_{eq} was achieved. Evidently, after long times of crystallization, two different types of crystals were present in the blends under some crystallization conditions, i.e., CB/soybean oil blend in Figures 3D,E, and CB/canola oil blend in Figures 4B,D,E. Based on the melting thermograms (Fig. 1B) and the analysis of the PLM video recordings, the small crystals were associated with the β′ polymorph and the large crystals with the β polymorph. Particularly large β crystals were developed in the CB/soybean oil blend at 13.5°C (Fig. 3E) and in the CB/canola oil blend at 13.0°C (Fig. 4B). The development of these large β crystals in both blends was associated with a significant increase in their melting temperature (i.e., T_{P2}, Table 1). It is well known that CB crystallized at different temperatures may develop the same polymorphic state, but with different crystal size and shape. However, it is important to point out that the common crystal morphology observed with pure CB (12,15) was not obtained in the blends studied here (Fig. 3). The main reason for this was the lower viscosity present in the blends (i.e., 1.14 and 0.95 Pa·s for CB/canola oil blend at 9.5 and 13.0°C, respectively; 1.03 and 0.80 Pa·s for CB/soybean oil blend at 10.0 and 13.5°C, respectively) in comparison with the higher viscosity of the CB melt. Crystallization in the blends occurred under lower limitations of mass transfer than crystallization in CB, resulting

TABLE 1
Melting Temperatures (T_M' and T_{P2}, see Fig. 1B), Solid Fat Content at Equilibrium (SFC_{eq}), Avrami Index (*n*), Fractal Measurement (*D*), and Pre-exponential Term of the Fractal Measurement [log(γ)] for the 30% Cocoa Butter (CB)/Vegetable Oil Blends at Different Crystallization Temperatures (T_{Cr})

T_{Cr}	T_M' (°C)	T_{P2}	SFC_{eq} (%)	$z \times 10^{-7}$ (min^{-n})	n^b	*D*	log(γ) (Pa)
30% CB/canola oil[a]							
9.5	21.4 (0.4)[b]	27.5 (1.5)[b]	24.4 (0.5)[b]	352.7 (15.5)[b]	2.82 (0.39)[b,*]	2.84 (0.00)[b]	–0.990 (0.080)[b]
10.5	21.9 (0.4)[c]	27.3 (1.3)[b]	23.6 (0.1)[c]	4.76 (0.273)[c]	3.44 (0.11)[c,*]	2.80 (0.05)[b]	0.297 (0.663)[c]
11.5	22.4 (0.2)[d]	27.1 (0.6)[b]	22.5 (0.2)[d]	1.42 (0.195)[d]	3.59 (0.44)[c,**]	2.45 (0.04)[c]	4.016 (0.989)[d]
13.0	23.1 (0.8)[e]	29.8 (0.1)[c]	20.7 (0.4)[e]	0.030 (0.002)[e]	3.60 (0.04)[c,**]	1.66 (0.37)[d]	5.459 (0.154)[d]
30% CB/soybean oil[a]							
10.0	19.8 (0.1)[b]	26.3 (0.8)[b]	26.3 (1.0)[b]	102.1 (12.4)[b]	3.34 (0.26)[b,*]	2.79 (0.02)[b]	–0.231 (0.470)[b]
11.0	20.8 (1.1)[b]	26.9 (0.3)[b]	25.2 (0.9)[b]	19.41 (1.07)[c]	3.25 (0.20)[b,*]	2.77 (0.02)[b]	–0.012 (0.202)[b]
12.0	22.3 (0.7)[c]	27.3 (0.5)[b]	24.2 (0.9)[c]	31.20 (4.39)[d]	3.42 (0.81)[b,**]	2.78 (0.01)[b]	0.552 (0.078)[c]
13.5	23.4 (0.2)[d]	29.1 (0.1)[c]	22.1 (0.4)[d]	0.024 (0.001)[e]	4.16 (0.25)[c,**]	2.76 (0.01)[c]	1.139 (0.001)[d]

[a]All measurements represent the mean ± SD of at least two independent determinations.[b,c,d,e]Within each column and for each CB/vegetable oil blend, values with the same letter are statistically the same ($P = 0.05$). A different letter indicates statistical difference ($P < 0.05$). T_M', experimental melting temperature of the β′ polymorph crystallized at a particular T_{Cr}; T_{P2}, experimental melting temperature of the β polymorph.
[b]Asterisk (*): instantaneous nucleation as shown by the video recordings. Double asterisks (**): sporadic nucleation as shown by the video recordings.

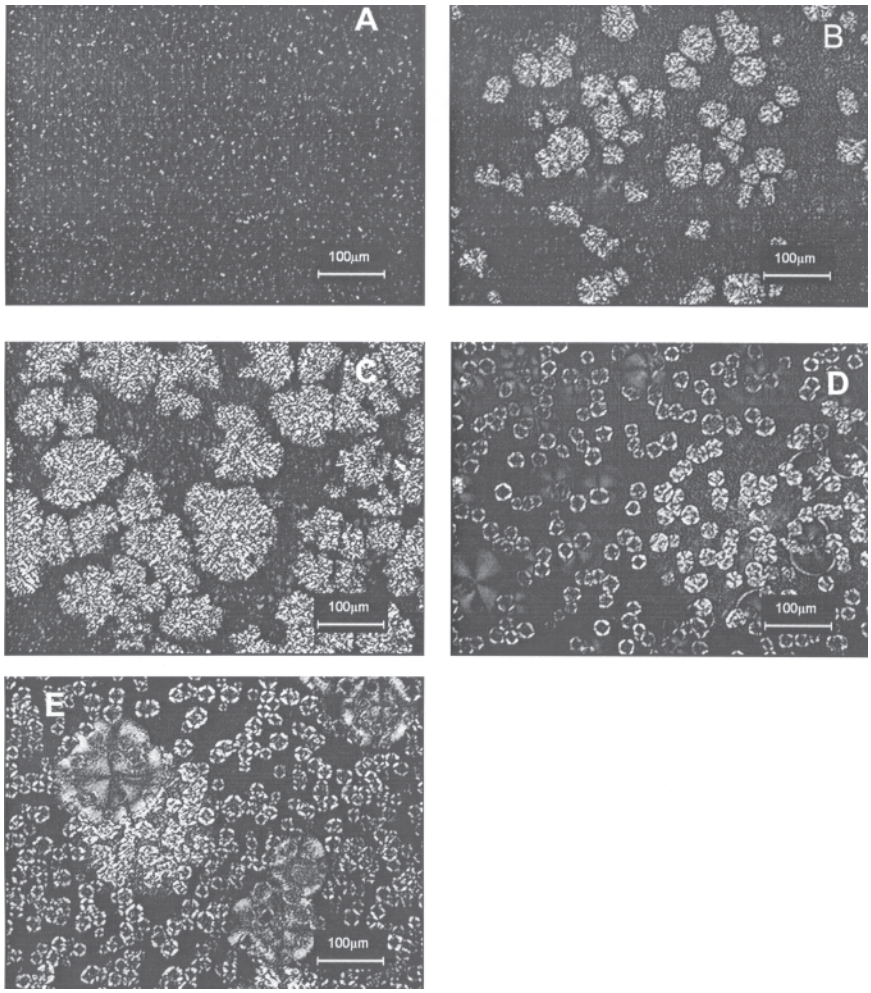

FIG. 3. Polarized light photomicrographs for the 30% cocoa butter/soybean oil blend crystallized at 10.0°C for 10 (A) and 80 min (B), and crystallized at 11.0°C for 190 min (C), at 12.0°C for 220 min (D), and at 13.5°C for 490 min (E).

in different crystal morphology and size from the ones commonly observed in CB.

The crystallization rate constant, z, is a complex rate constant dependent on the value of n (i.e., the units of z are min^{-n}, Table 1). However, in the CB/vegetable oil blends investigated, the n value varied within a relatively small interval, thus limiting the dependence of z on the n value. The T_{Cr} effect on z was evaluated with the Arrhenius equation. The statistical analysis was done through the General Linear Model procedure available in STATISTICA. The results showed that each CB/vegetable oil blend was described by an independent Arrhenius equation ($P = 0.10$) (data not shown). Then, as T_{Cr} increased, higher values of z were obtained with the CB/soybean oil blend than with the CB/canola oil blend (Table 1). The overall crystallization process, including nucleation and crystal growth, occurred at a faster rate in the system with higher supercooling conditions (CB/soybean oil) than in the system with lower supercooling conditions (CB/canola oil). These observations agreed with the SFC_{eq} results previously discussed. However, the differential effect of $(T_{Cr} - T_M^{\circ})$ was not observed in the behavior of n, since, as already indicated, the TAG of CB followed a spherulitic crystal growth mechanism in the blends with vegetable oils, independent of the blend and the T_{Cr}.

Fractal dimension in the CB/vegetable oil blends. The fractal dimension, D, and the corresponding pre-exponential factor [log(γ)] for the CB/vegetable oil blends at the different T_{Cr} values are shown in Table 1. Note that D is a parameter associated with the dimensionality of the crystal network structure, and log(γ) is a constant that is dependent on the size of the primary particles and the interactions between them (i.e., polymorphic nature of the crystals) but that is independent of the solid fraction, SFC (2). The log(G') vs. log(SFC) curves describe the evolution of the fractal organization as CB crystallization proceeds at the different T_{Cr} values investigated. Different slopes were observed as crystallization continued (data not shown). These slopes were associated with the different stages of organization, which were gradually accomplished by the TAG crystals as a function of crystallization time until a plateau was achieved. Similar results were obtained with blends of palm stearin in sesame oil (9) and with pure CB (12). The linear regression of log(G') on log(SFC) before achieving the plateau was used to determine D and log(γ). This regression provided

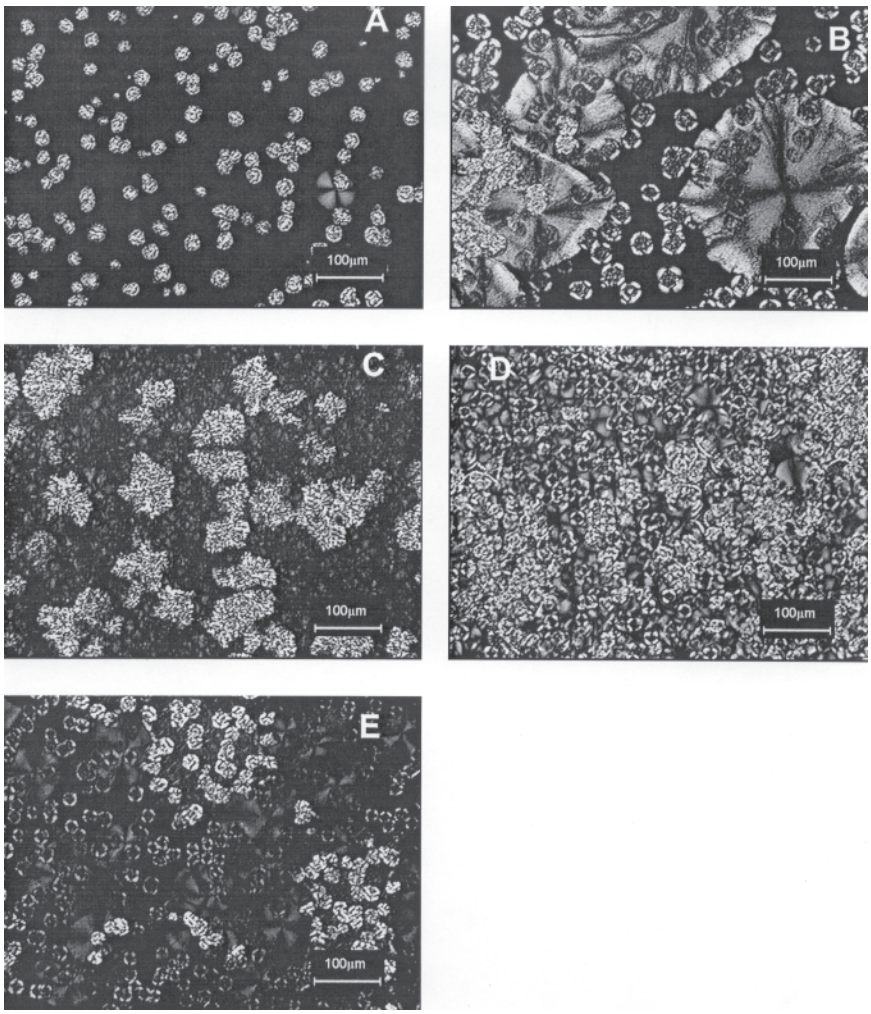

FIG. 4. Polarized light photomicrographs for the 30% cocoa butter/canola oil blend crystallized at 13.0°C for 100 (A) and 450 min (B), and crystallized at 9.5°C for 100 min (C), at 10.5°C for 120 min (D), and at 11.5°C for 190 min (E).

coefficients of determination (r^2) larger than 0.98 ($P < 0.025$) in all cases. Thus, similar D values ($P = 0.05$) were obtained with the CB/soybean oil blends at 10.0, 11.0, and 12.0°C (Table 1). Under these conditions, the average D value for the T_{Cr} values used was 2.78 (±0.01). This similar D value was obtained despite the fact that crystals with different sizes and shapes formed the corresponding crystal network structures in the CB/soybean oil blend. This situation was even more evident under conditions where SFC_{eq} was reached (Fig. 3B–D). In contrast, at 13.5°C we obtained a lower D value [2.76 (±0.01)] ($P < 0.05$) (Table 1), which corresponded to a less compact 3-D crystal network structure (Fig. 3E) than the one developed at 12.0°C (Fig. 3D), and particularly to the ones developed at 10.0 (Fig. 3B) and 11.0°C (Fig. 3C). On the other hand, in the CB/canola oil blend, the system, where lower supercooling conditions existed, the D values decreased as T_{Cr} increased ($P < 0.05$). In this system, the D values were associated with differences in crystal sizes and shapes and in the organization of the corresponding crystal network structure. As with the CB/soybean oil blend, this situation was even more evident under apparent crystallization equilibrium (i.e., SFC_{eq} was reached) (Fig. 4B–E). Regarding log(γ), the statistical analysis showed that as T_{Cr} increased, the CB/canola oil blend achieved larger log(γ) values than the CB/soybean oil blend ($P < 0.05$) (Table 1). Previous research showed that log(γ) is a more sensitive parameter than D to use to establish differences in crystal size and shape, and in crystal network organization (12). The foregoing results showed that, although similar T_{Cr} values were used, their effect on the organization of the 3-D crystal network [i.e., D and log(γ)] was different in each blend. Unfortunately, we could not find any relationship between D or log(γ) and the dimensionality of crystal growth (n), $T_{M'}$ or T_{P2}.

In general, in the CB/vegetable oil blends, β crystals grew larger than β′ crystals; in the CB/canola oil blend at 13.0°C, the average diameter of β′ crystals was 41.4 μm (±4.6) and of the β crystals was 274.0 μm (± 66.6)]. When large β crystals were present in the crystal network, such as in the CB/canola oil blend at 13.0°C, the result was an increment in the T_{P2} value (Table 1) and the development of a less compact 3-D crystal network structure ($D = 1.66 \pm 0.37$; Fig. 4B) than the ones

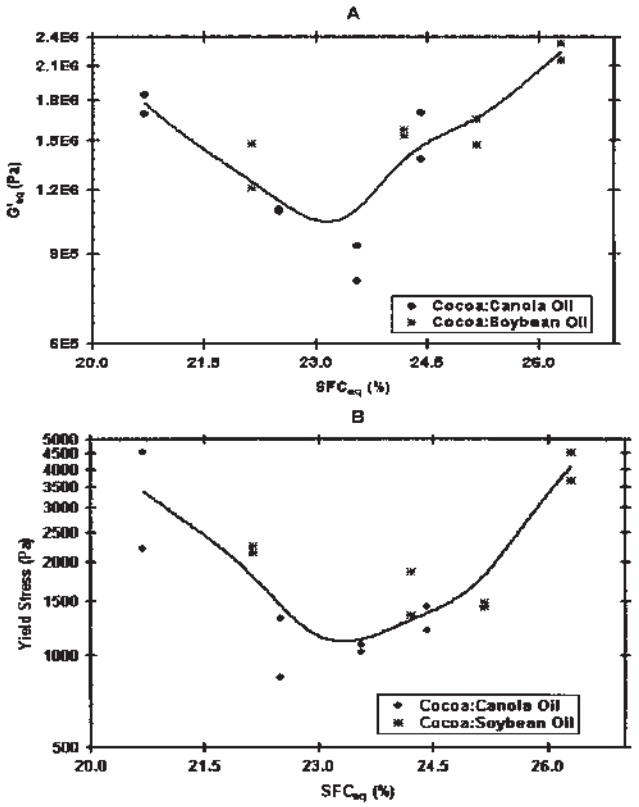

FIG. 5. Equilibrium elasticity, G'_{eq} (A), and yield stress, σ* (B), as a function of equilibrium solid fat content, SFC_{eq}, for the 30% cocoa butter (CB)/soybean oil and the 30% CB/canola oil blends. The lines represent the least squares fitting of the data.

developed at lower temperatures (Fig. 4C–E). A similar increase in the T_{P2} value was also observed in the CB/soybean oil blend crystallized at 13.5°C, and large β crystals were also observed in the PLM photomicrographs (Fig. 3E); in the CB/soybean oil blend at 13.5°C, the average diameter of β′ crystals was 33.2 μm (±2.9) and for the β crystals was 133.2 μm (±32.3)]. However, such an increase in T_{P2} was matched by a small, but significant, decrease in the *D* value (Table 1). Apparently, the presence of β crystals had a more significant effect in the structural organization of the crystal network developed in the CB/canola oil blend than the one developed in the CB/soybean oil blend. The larger log(γ) observed for the CB/canola oil blend (Table 1) might be associated with the larger β crystals developed in this system in comparison with the size of β crystals developed in the CB/soybean oil blend.

Behavior of G'_{eq} and σ in the CB/vegetable oil blends.* G'_{eq} and σ* were measured in the crystallized CB blends once the SFC_{eq} had been reached (Figs. 3B–E; 4B–E). This situation represented the point where the increase in crystal mass (i.e., increase in the SFC) just resulted in coarsening of the crystal network without without affecting the overall 3-D distribution of the crystal mass previously developed (3). Within this framework, Marangoni's group (17,18) has shown that the elastic and yield behaviors of fat crystal networks are associated with how much material forms the network (SFC_{eq}), its 3-D structure (*D*), and the interfacial forces between the solid and the liquid phases through the crystal network. The behaviors of G'_{eq} and σ* as a function of SFC_{eq} for each blend are shown in Figures 5A and 5B, respectively. The lines of fit in these graphs show the generalized behavior of G'_{eq} and σ* values as a function of SFC_{eq}, i.e., independent of the CB/vegetable oil blend. However, this did not mean that the generalized behavior of G'_{eq} and σ* was independent of $T_M°$, since there was a supercooling effect associated with the magnitude of SFC_{eq}. Thus, considering the $T_M°$ of the CB blends, the greatest values of both G'_{eq} and σ* parameters were achieved at the highest and lowest supercooling conditions investigated, i.e., CB/soybean oil at 10.0°C and CB/canola oil at 13.0°C, respectively (Fig. 5A,B). Such G'_{eq} and σ* values corresponded to the highest and lowest SFC_{eq} levels in the blends, respectively (Table 1). At intermediate SFC_{eq} values, the blends had lower G'_{eq} and σ* values (Fig. 5A,B). Thus, the generalized G'_{eq} and σ* behavior showed two regions. In the first, G'_{eq} and σ* decreased as SFC_{eq} increased between 20 and 23% (Figs. 5A,B). Independent of the blend used, this region was associated with crystal network structures formed by mixtures of small β′ crystals and large β crystals. The PLM photomicrographs that illustrate the decrease of G'_{eq} and σ* as SFC_{eq} increased correspond, respectively, to Figures 4B, 3E, and 4E. Thus, independent of the blend used, as SFC_{eq} increased in the interval within 20 to 23%, the size of β crystals decreased and the crystal network structure became denser as G'_{eq} and σ* decreased. This relationship between the rheological parameters and the SFC_{eq} is peculiar and will be discussed shortly.

In the second region, G'_{eq} and σ* followed a direct relationship with SFC_{eq} that was independent of the blend used (Fig. 5A,B). The PLM photomicrographs that document the increase in G'_{eq} and σ* as SFC_{eq} increased between 24 and 27% correspond, respectively, to Figures 3D, 4C, 3C, and 3B. In this region the presence of β crystals was evident only in the crystal network structure developed at 12.0°C in the CB/soybean oil blend (Fig. 3D). The rest of the crystallizing conditions developed crystal network structures formed mainly by aggregates of small β′ crystals (Figs. 4C, 3C, and 3D). The lower elasticity value that established the border between the first and second region of the G'_{eq} behavior (Fig. 5A) corresponded to the CB/canola oil blend crystallized at 10.5°C with $D = 2.80$ and SFC_{eq} of 23.6% (Table 1, Fig. 4D). The corresponding plot for the generalized behavior of σ* (Fig. 5B) also showed a minimum at these crystallizing conditions. Above 10.5°C, we observed a significant increment in the log(γ) value for the CB/canola oil blend (i.e., 11.5 and 13.0°C, Table 1). As previously indicated, this increment in log(γ) was associated with the development of large β crystals in this blend (Fig. 4C,B).

A polymorphic transition was associated with the change in G'_{eq} and σ* behavior between the first and second regions (Fig. 5). A similar polymorphic transition for the CB/soybean oil blend occurred at 12.0°C (Table 1, Fig. 3D). This polymorphic transition was also associated with an increase in log(γ) and the development of large β crystals above this T_{Cr} (13.5°C, Fig. 3E). However, the increase in log(γ) was not so large as the one observed in the CB/canola oil blend (Table 1) mainly because β crystals did not grow as large in the CB/soybean oil blend as

in the CB/canola oil blend. The polymorphic transitions occurring in each blend were associated with modifications in the spatial distribution of the crystal network as evaluated by PLM. However, we could not find a particular relationship that described the generalized behavior of G'_{eq} and σ* as a function of *D* and independent of the CB/vegetable oil blend. Nevertheless, some results might be described within this framework. Considering the T_M° values, we observed that the higher ($T_{Cr} - T_M^\circ$) values for each blend were present in the second region. As a result, dense crystal network structures with similar *D* values [2.84 (±0.00) at 9.5°C with CB/canola oil and 2.78 (±0.01) with CB/soybean oil at 10.0, 11.0, and 12.0°C] were formed mainly by aggregates of small β′ crystals. Then, for a rather constant value of *D,* the increase in G'_{eq} and σ* might be associated more with the increase in SFC_{eq} (Fig. 5). The behavior of the first region is more difficult to explain since, as SFC_{eq} decreased, loosely packed crystal network structures were developed (Figs. 4E, 3E, and 4B) with higher G'_{eq} and σ* values (Fig. 5). In this region the lower ($T_{Cr} - T_M^\circ$) conditions within each blend were present, resulting in crystallized systems formed by mixtures of small β′ and large β crystals. As the β crystals became larger and SFC_{eq} decreased, the small β′ crystals filled the spaces among the large β crystals (Figs. 3E and 4B). The small β′ crystals might be acting as binder particles, increasing the surface area for van der Waals forces among large β crystals, providing structural characteristics (elasticity and yield stress) to crystal networks with low SFC_{eq} and *D* values (Fig. 5, Table 1). However, large G'_{eq} and σ* values were not always achieved by crystallized systems formed by mixtures of small β′ crystals and large β crystals (10.5 and 11.5°C CB/canola oil blend, Fig. 4D,E). It seems that the occurrence of the cooperative structural effect requires an appropriate proportion of β′ and β crystals and the right crystal size ratio between the β′ and β crystals. An additional variable affecting G'_{eq} and σ* is the interaction forces associated with the van der Waals forces between the structural elements of the network, which in turn depend on the shape of the clusters of crystals (17). No direct measurement of this variable was made in the systems evaluated in the present investigation. However, the relevance of such forces and their effect on G'_{eq} and σ* of the crystal network have to be considered in light of its strong dependence on the shape of the cluster of crystals forming the network (17), particularly when we consider that such shapes might not be homogeneously distributed through the crystal network (Figs. 3E, 3D, 4B, and 4E). On the other hand, through mathematical simulation Marangoni and Rogers (18) showed that, assuming a fixed crystal size, the lower the *D* value is, the higher the yield stress. In the same way, they reported that for a fixed *D* value, the larger the primary crystal size is, the lower the value of σ*. However, these situations are difficult to extrapolate to actual experimental conditions where several variables interact to determine σ* in crystallized systems. Finally, it is important to point out that the mechanical properties of the crystal network structures developed in both CB/vegetable oil blends at all T_{Cr} values were strong enough to withstand collapse, and no free oil was released even after 60 min of centrifugation at 25, 000 × *g*.

ACKNOWLEDGMENT

This research was supported by Consejo Nacional de Ciencia y Tecnología through grant 2002-C01-39897.

REFERENCES

1. deMan, J.M., and L. deMan, Texture of Fats, in *Physical Properties of Lipids*, edited by A.G. Marangoni and S.S. Narine, Marcel Dekker, New York, 2002, pp. 191–217.
2. Narine S.S., and A.G. Marangoni Fractal Nature of Fat Crystal Networks, *Phys. Rev. E 59*:1908–1920 (1999).
3. Marangoni, A.G., The Nature of Fractality in Fat Crystal Network, *Trends Food Sci. Technol. 13*:37–47 (2002).
4. Hoffman, J.D., and J.J. Weeks, Melting Process and the Equilibrium Melting Temperature of Polychlorotrifluoroethylene, *J. Res. Natl. Bur. Std. 66*:13–28 (1962).
5. Toro-Vazquez, J.F., M. Briceño-Montelongo, E. Dibildox-Alvarado, M.A. Charó-Alonso, and J. Reyes-Hernández, Crystallization Kinetics of Palm Stearin in Blends with Sesame Seed Oil, *J. Am. Oil Chem. Soc. 77*:297–310 (2000).
6. Liu J.-W., S. DeMichele, M. Bergana, E. Bobik Jr., C. Hastilow, L.-T. Cuang, P. Mukerji, and Y.-S. Huang, Characterization of Oil Exhibiting High γ-Linolenic Acid from a Genetically Transformed Canola Strain, *Ibid. 78*:489–493 (2001).
7. O'Brien, R.D., *Fats and Oils, Formulating and Processing for Applications*, Technomic Publishing, Lancaster, PA, 1998, pp. 1–44.
8. Sonntag, N.O.V., *Bailey's Industrial Oil and Fat Products*, 4th edn., edited by D. Swern, John Wiley & Sons, New York, 1982, Vol. 2, pp. 407–525.
9. Toro-Vazquez, J.F., E. Dibildox-Alvarado, M.A. Charó-Alonso, V. Herrera-Coronado, and C.A. Gómez-Aldapa, The Avrami Index and the Fractal Dimension in Vegetable Oil Crystallization, *J. Am. Oil Chem, Soc. 79*:855–866 (2002).
10. Norton, I.T., C.D. Lee-Tuffnell, S. Ablett, and S.M. Bociek, Calorimetric, NMR and X-ray Diffraction Study of the Melting Behavior of Tripalmitin and Tristearin and Their Mixing Behavior with Triolein, *Ibid. 62*:1237–1244 (1985).
11. Toro-Vazquez, J.F., and A. Gallegos-Infante, Viscosity and Its Relationship to Crystallization in a Binary System of Saturated Triacylglycerides and Sesame Seed Oil, *Ibid. 73*:1237–1246 (1996).
12. Toro-Vazquez, J.F., D. Pérez-Martínez, E. Dibildox-Alvarado, M. Charó-Alonso, and J. Reyes-Hernández, Rheometry and Polymorphism of Cocoa Butter During Crystallization Under Static and Stirring Conditions, *Ibid. 81*:195–203 (2004).
13. van Malssen, K., A. van Langevelde, R. Peschar, and H. Schenk, Phase Behavior and Extended Phase Scheme of Static Cocoa Butter Investigated with Real-Time X-ray Powder Diffraction, *Ibid. 76*:669–676 (1999).
14. Gibon, V., F. Durant, and Cl. Deroanne, Polymorphism and Intersolubility of Some Palmitic. Stearic, and Oleic Triglycerides: PPP, PSP, POP, *J. Am. Oil Chem. Soc. 63*:1047–1055 (1986).
15. Sharples, A., *Introduction to Polymer Crystallization*, Edward Arnold, London, 1966, pp. 44–59.
16. Marangoni, A.G., and S.E. McGauley, Relationship Between Crystallization Behavior and Structure in Cocoa Butter, *Crystal Growth Design 3*:95–108 (2002).
17. Marangoni, A.G., Elasticity of High-Volume-Fraction Fractal Aggregate Networks: A Thermodynamic Approach, *Phys. Rev. B 62*:13951–13955 (2000).
18. Marangoni, A.G., and M.A. Rogers, Structural Basis for the Yield Stress in Plastic Disperse System, *Appl. Phys. Lett. 82*:3239–3241 (2003).

[Received November 23, 2004; accepted May 29, 2005]